Journal of Nanobiotechnology

RESEARCH

Open Access

Manipulation in root-associated microbiome via carbon nanosol for plant growth improvements

Lingtong Cheng[1,2], Jiemeng Tao[1,2], Peng Lu[1,2], Taibo Liang[3], Xutao Li[4], Dong Chang[4], Huan Su[1,2], Wei He[5], Zechao Qu[2], He Li[2], Wenjun Mu[1,3], Wei Zhang[6], Nan Liu[6], Jianfeng Zhang[1,2], Peijian Cao[1,2,7*] and Jingjing Jin[1,2*]

Abstract

Background Modulating the microbiome with nanomaterials has been proposed to improve plant growth, and reduce reliance on external inputs. Carbon Nanosol (CNS) was attracted for its potential to improve plant productivity. However, the mechanism between CNS and rhizosphere microorganisms remained largely elusive.

Results Here, we tried to systematically explore the effects of CNS (600 and 1200 mg/L by concentration) on tobacco growth, soil physical properties, and root-associated microbiome. The influence of CNS on soil physicochemical properties and plant growth was significant and dose-dependent, leading to a 28.82% increase in biomass accumulation by 600 mg/L CNS. Comparison between the CNS-treated and control plants revealed significant differences in microbiome composition, including 1148 distinct ASVs (923 bacteria and 225 fungi), microbiome interactions, and metabolic function of root-associated microbiomes. Fungal and bacterial communities had different response patterns for CNS treatment, with phased and dose-dependent effects, with the most significant changes in microbial community structure observed at 1200 mg/L after 10 days of treatment. Microbial networks of CNS-treated plants had more nodes and edges, higher connectivity, and more hub microorganisms than those of control plants. Compared with control, CNS significantly elevated abundances of various bacterial biomarkers (such as *Sphingomonas* and *Burkholderia*) and fungi biomarkers (including *Penicillium*, *Myceliophthora*, and *Talaromyces*), which were potential plant-beneficial organisms. Functional prediction based on metagenomic data demonstrated pathways related to nutrient cycling being greatly enriched under CNS treatment. Furthermore, 391 culturable bacteria and 44 culturable fungi were isolated from soil and root samples. Among them, six bacteria and two fungi strains enriched upon CNS treatment were validated to have plant growth promotion effect, and two fungi (*Cladosporium* spp. and *Talaromyces* spp.) played their roles by mediating volatile organic compounds (VOCs). To some extent, the driving and shaping of the microbiome by CNS contributed to its impact on plant growth and development.

Conclusion Our results revealed the key role of root-associated microbiota in mediating the interaction between CNS and plants, thus providing valuable insights and strategies for harnessing CNS to enhance plant growth.

Keywords Carbon nanosol, Plant growth-promoting rhizobacteria, Plant growth, Microbiome, Engineered nanomaterials

*Correspondence:
Peijian Cao
peijiancao@163.com
Jingjing Jin
jinjingjing1218@126.com
Full list of author information is available at the end of the article

Graphical Abstract

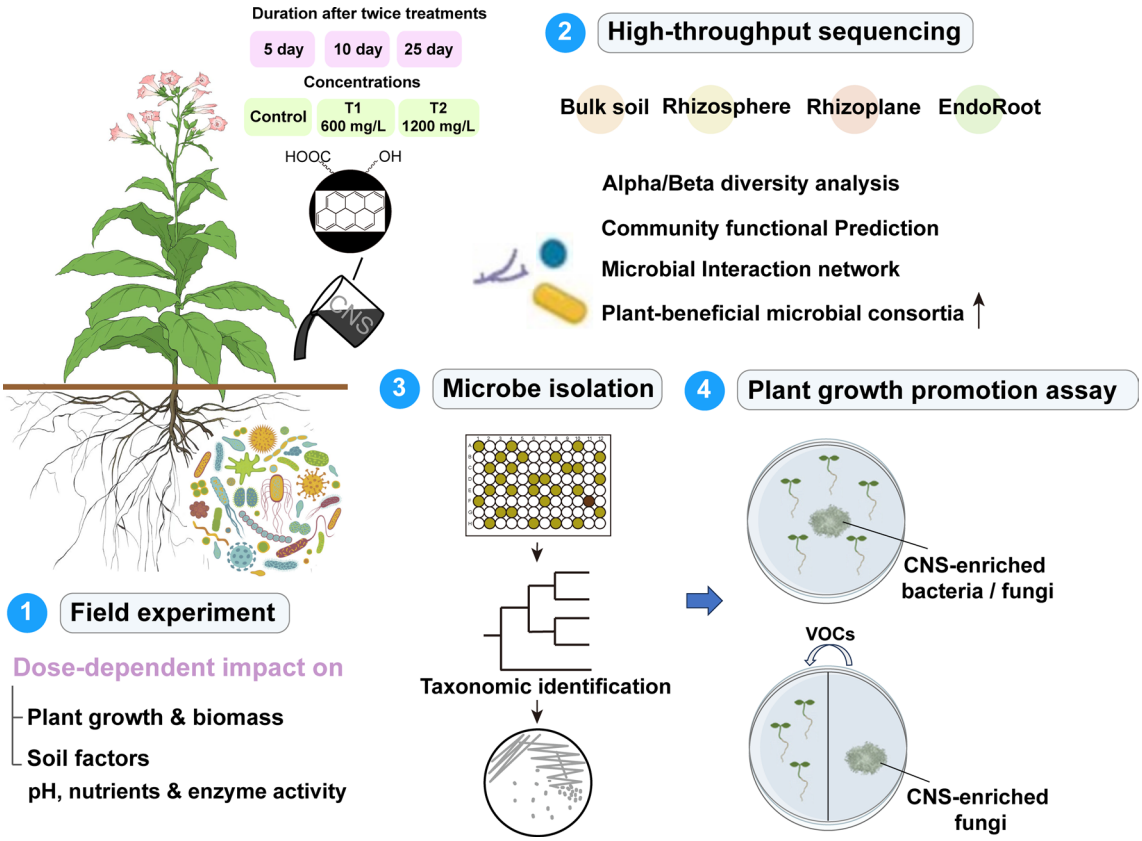

Background

The root-associated microbial community, as an extraordinarily intricate ecological system, endowed with numerous beneficial traits which were capable of modulating plant growth under various a/biotic stress [1]. The judicious usage of beneficial microorganisms held promise in reducing usage of pesticides and synthetic fertilizers, thereby providing potential avenues for enhancing plant growth and health [2]. Plant Growth-Promoting Rhizobacteria (PGPR) or Plant Growth Promoting Fungi (PGPF) were a wide range of microorganisms that colonized the plant rhizosphere with plant growth-promoting and disease-suppressing properties. PGPR enhanced plant growth by producing plant growth regulators through various mechanisms, including mobilization of nutrition in the soil (phosphate solubilization [3], nitrogen fixation [4], and iron chelation [5]), regulating plant hormones (the production of 1-aminocyclopropane-l-carboxylate deaminase (ACC deaminase) [6] and synthesis of plant hormones [7]), emission of volatile organic compounds (VOCs) or activating the plant physiological protection system[2, 8].

With the advancement of nanotechnology, nano-enabled approaches were expected to offer a sustainable platform for plant growth through regulating plant microbiome in agroecosystems [9, 10]. The utilization of engineered nanomaterials (ENMs) in agricultural microbiome engineering to improve plant health and productivity had been initially explored [11]. For instance, CeO_2 ENMs strengthened maize salt stress resistance (86.8%) and improved crop yield by enhancing the abundance of salt-tolerant PGPRs, such as *Flavobacterium, Sphingomonas*, and *Allochromatium* [12]. Chitosan-iron nanocomposite exposure led to a notable decrease in the relative abundance of *Xanthomonas oryzae pv. oryzae*, a pathogenic bacterium in rice, while preserved the beneficial structure of the endophytic bacterial community in rice [13]. Wang et al. revealed that Se nanoparticles elevated the relative abundance of some PGPRs of *Brassica chinensis L.*, leading to enhanced yield and photosynthetic efficiency of crops [14]. Copper oxide

nanoparticles at 50 mg/L reshaped the microbiome of nitrogen utilization in wheat, thereby bolstering plant health and nitrogen efficiency [15]. Moreover, when maize plants were subjected to 50 mg/L of iron oxide (FeO) nanoparticles, the abundance of genera such as *Pantoea*, *Burkholderia-Paraburkholderia*, *Nocardioides*, *Chitinophaga sancti*, and *Rhizobium*, were significantly increased. These genera have known associations with plant growth promotion and carbon cycling [16]. Similarly, the addition of molybdenum disulfide nanoparticles at 100 mg/L in rice enhanced beneficial soil microbes like *Bacillus* and *Nostoc*, resulting in a growth increase of 6.8–7.9%, along with elevated nutrient utilization, and photosynthetic enzymes by 30% [17]. Therefore, ENMs had the potential of improving plant performance as well as different a/biotic stress resistance in various crops by modifying plant-associated microbiome [18–20].

While nanomaterials (NMs) had significant potential for promoting plant growth, the responses were dose-dependent and could lead to phytotoxicity in crops if not used correctly [21, 22]. Typically, many studies have demonstrated that ENMs could activate various physiological function of plants at relative low concentration. For example, the growth of soybean could be improved by nano-CeO_2 at a dose of 250 mg/L [23]. However, the application of 400 mg/L CeO_2 NMs did not promote biomass and yield of soybean, but decreased the chlorophyll content [24], which suggested that CeO_2 ENMs at a high dose might be a potential negative regulator on plants. Similarly, carbon-based nanomaterials also affected corn [25] and bean sprouts [26] growth in a concentration-dependent pattern, with growth promotion at low concentrations, and vice versa, respectively. In *Salvia verticillata L.*, multi-walled carbon nanotubes (MWCNTs) also played their roles in a dose-dependent effect, with oxidative stress indices improved in the leaves of plants [27]. Furthermore, numerous studies have reported that the effects of ENMs (Graphene oxide [28], Ag [29], TiO_2 [30] and ZnO Nanoparticles [31]) on microorganisms also exhibited dose-dependent tendencies. Thus, to some extent, the potential effects of ENMs on plant growth and microorganisms seemed to be dose dependent, necessitating further investigation to determine their optimal usage conditions.

Carbon nanosol (CNS), as a highly hydrophilic carbon-based nanomaterial, had potential application prospects in agriculture as it exhibited superior plant growth-promoting ability [32]. Previous studies had indicated that appropriate concentrations of CNS could enhance plant growth and increase plant potassium content [33]. The introduction of CNS also could enhance the growth of young tobacco seedlings in pot and hydroponic experiments [34]. Despite the promising capacity of CNS, the underlying mechanisms governing its growth-promoting effects and its modulation of the rhizospheric microbial environment remained unclear. In addition to promoting rice seedling growth at optimal concentrations, CNS might also provide broad-spectrum resistance for rice [35]. We have explored the effects of CNS on rhizospheric microorganisms under laboratory conditions [36], but its impact under natural conditions remains unknown. Hence, a comprehensive investigation extending to more extensive field experiments into the ecological implications of CNS on the rhizosphere microenvironment is needed. The aim of the current study was to elucidate the intricate interactions among CNS, plants and microorganisms, and the underlying mechanisms responsible for the growth-promoting effects of CNS. In this study, cultivated tobacco (*Nicotiana tabacum L.*) were exposed to three different concentrations of CNS (CK: 0 g/L, T1: 600 mg/L, and T2: 1,200 mg/L). We employed amplicon sequencing to explore the patterns of root-associated microbial communities at the 5th, 10th, and 25th days after the application of CNS. Additionally, metagenomic analysis was conducted to explore the functional roles of the microbiota under CNS treatment. We then isolated some strains and explored their roles in tobacco growth promotion. Our findings highlighted the pivotal role of rhizosphere microorganisms in mediating the interaction between CNS and plants, offering valuable insights and strategies for enhancing tobacco growth through CNS application.

Methods

Experiment design

Field experiments were conducted in 2022 at the Experimental Farm at Jiaxian (33°98′S, 113°19′E), Henan Province, China. The experimental site was characterized by cinnamon soil. During the growth period (from May to September), the average temperature ranged from 21.70℃ to 29.96℃, with total rainfall of 383 mm. Irrigation was applied twice, with approximately 30 cubic meters of water per application. The tobacco (*Nicotiana tabacum L.*) cultivar Zhongyan100 was chosen as the experimental material. After germination, individual one-month-old tobacco seedlings were transplanted into the field.

The preparation of CNS has been introduced in the previous method [37], and CNS was obtained from commercial company (Beijing Naisis New Material Technology)[38]. Our study consisted of three independent experiments (CK, T1, and T2), each with an area of about 100 m^2, and 150 tobacco plants were evenly planted. The two treatment groups represented applying CNS to the soil at two concentrations (T1: 600 mg/L, T2: 1200 mg/L), with a volume of 0.3 L per plant. After transplantation,

CNS was applied once a week for a total of two weeks. The control group (CK) received an equivalent amount of water. After the application of CNS for 5, 10, and 25 days, agronomic parameters including plant height, internode distance, stem diameter, leaf width, leaf length, and leaf count were measured. Five replicates were performed for each group.

Sample collection

Samples were collected after the application of CNS for 5, 10, and 25 days. Similar with previous studies [39], both control and CNS-treated plants were randomly selected from 8 different locations in the field to ensure representativeness. Bulk soil (BS) was removed from roots by shaking them vigorously. Rhizosphere soil (RS) was then separated from roots by shaking roots and soil. After cutting off the roots with disinfected scissors, they were wrapped in tin foil and stored with liquid nitrogen for further sample processing in laboratory. Simultaneously, the half of the bulk soil samples were analyzed for nutrients and extracellular enzyme potential activity. The root was put in in a 50 mL centrifuge tube for 5 min at 600 rpm (Vortex-Genie2 Mixers SI-0256, USA). Next, the soil suspension was further processed for 15 min at 4000 g. The obtained soil pellet was considered as rhizoplane soil (RP). Roots were then transferred to a new tube for subsequent procedures. Using distilled water, roots were thoroughly washed, followed by surface sterilization to remove microbes on the surface by shaking roots in 25 mL of 75% alcohol solution for 5 min at 200 rpm. Then, after washing three times with sterile phosphate buffer, the grinding step was applied to the roots to obtain a fine powder. The final wash was inoculated on a nutrient agar plate at 37 °C for 2d. No viable colonies were observed, which demonstrated the effectiveness of the disinfection procedure. These treated roots were used for root endosphere (R) extraction. All samples were then stored at -80 °C until DNA extraction and microbial isolation.

Soil nutrients and extracellular enzyme activity measurement

Soil moisture was measured gravimetrically. The potentiometric method was applied to measure soil pH in a 1:1 soil–water mixture. Total potassium (TK) and total phosphorus (TP) were digested with NaOH, whereas total nitrogen (TN) was measured by micro-Kjeldahl digestion followed by steam distillation. We employed steam distillation and indophenol-blue colorimetry method to measure nitrate nitrogen (NN) and ammonium nitrogen (AN), respectively. Soil samples were first extracted using $NaHCO_3$, and available soil phosphorus (AP) was determined using molybdate-blue colorimetry. For measurement of soil potassium (AK), ammonium acetate was used to extract soil samples, and the extracts were loaded onto an atomic absorption spectrometer with ascorbic acid as a reductant.

Acid phosphatase activity (Apase) of soil sample was determined by phenylene disodium phosphate colorimetry method. Enzymes including disaccharide cellulase (CBH), beta-1,4-glucosidase (BG), and leucine aminopeptidase (LAP) were determined by fluorometric quantification [40]. Sucrase (SC) activity was determined using the 3,5-dinitrosalicylic acid colorimetric method, and peroxidase (POD) and polyphenol oxidase (PPO) activities were determined by the colorimetric method using pyrogallic acid. All samples were analyzed three times. A two-tailed t-test was adapted to determine the statistical significance between CNS-treated groups and the control group (CK). Results with p-values less than 0.05 were considered statistically significant, and all analyses were performed using R.

Amplicon sequencing and analysis

A total of 216 samples (3 treatments × 6 replicates × 4 niches × 3 stages) were used for amplicon sequencing. Total DNA was obtained from soil and root samples by the Mag-Bind Soil DNA Kit (Omega Biotek, Doraville, GA, USA). Universal primers 515F (5′-GTGCCA GCMGCCGCGGTAAT-3′) and 806R (5'-GGACTA CHVGGGTWTCTAA-3') were applied to the amplification of bacterial 16S rRNA gene V4 region. Additionally, the fungal ITS1 region amplicon sequencing was performed with the primer sets ITS1F (5'-CTTGGT CATTTAGAGGAAGTAA-3') and ITS2 (5'-GCTGCG TTCTTCATCGATGC-3'). Table S6 showed the PCR system and amplification conditions. The MiSeq platform of Novogene Technology Co. Ltd (Tianjin, China) was applied to high-throughput sequencing. Bacterial and fungal sequences were clustered using SILVA (v13.2) [41] and UNITE (v8.0) [42] databases, respectively. We removed bacterial ASVs assigned to chloroplast and mitochondrial. In order to avoid possible biases, we also filtered bacterial and fungal ASVs covered by less than 2 sequences. Finally, 21,921,510 bacterial and 20,193,010 fungal high-quality reads with an average of 78,854 and 72,118 reads per sample were retrieved, which were sorted into 5,430 bacterial and 1,448 fungal amplicon sequence variants.

Metagenomic sequencing and analysis

A total of 24 samples (2 treatments × 3 replicates × 4 niches × 1 stage) were used for metagenomic sequencing. The extracted DNA for amplicon sequencing was also used for metagenomics sequencing on an Illumina

HiSeq platform with 150 bp paired-end reads by Novogene Technology Co. Ltd (Tianjin, China).

The raw reads were removed using FastQC (v0.23.1) with a minimum Q Score of 20 and a maximum containing undetermined bases (N) of 10. MetaSPAdes was applied to assemble the clean reads into scaffolds with default parameters [43]. Open reading frames (ORFs) prediction was conducted to scaffolds bigger than 500 bp using prokka (v0.43). After filtering redundant genes, a non-redundant initial gene set was obtained. Genes with similarity > 95% were clustered, with the longest gene in each cluster serving as the representative gene sequence. Alignment between assembled genes and raw sequencing reads yielded gene counts for each sample. Genes with an average coverage below 2 were filtered, resulting in a gene set for subsequent analysis. Statistical analysis was conducted using the gene abundance of each sample. The eggNOG database (v5.0) [44] and Kyoto Encyclopedia of Genes and Genomes (KEGG) database (release 80.1) using DIAMOND (v0.922.123) [45], was used for functional analysis of the non-redundant gene catalog, with an E-value cutoff of 1e − 5. Plant growth promotion related genes were also searched, including the production of indole acetic acid (IAA); nitrogen and sulfur metabolism; suppression of pathogenic fungi, and so on (Table S7).

Network construction and analysis

Molecular ecological networks (MENs) were determined using Spearman correlations among ASVs, and a random matrix theory (RMT)-based method was used to measure the correlation cut-off threshold in a non-arbitrary way. Networks were inferred for soil and root communities using ASV relative abundances at each time point. During network construction, only ASVs detected in more than half of the replicate samples were used. We used RMT to automatically determine the appropriate similarity threshold (St) prior to network construction. The properties of global network were characterized according to Deng et al. [46]. All analysis were performed using the Molecular Ecological Network Analysis (MENA) tool (http://ieg2.ou.edu/MENA/) [47], and networks were graphed by gephi 0.8.2-beta [48].

Isolation and identification of the tobacco microbes

Using the methodology established by Zhang et al., the isolation and identification of individual bacteria were carried out using the limited dilution technique in a 96-well cell culture plate [49]. It involved dispersing a single bacterium into the liquid medium and subsequently amplifying 16S rRNA gene using the V5-V7 region with a unique barcode for identification. For the isolation of fungi, a gram of root combined with rhizosphere soil treated with CNS was finely fragmented and homogenized using autoclaved glass beads within a 2 mL centrifuge tube. The mixture was subjected to serial dilution in sterile phosphate buffer (5.0 mL) and subsequent spread plating of 150 µl aliquots from dilutions ranging between 10^{-4} and 10^{-7} onto streptomycin-containing Potato Dextrose Broth (PDB) plates to facilitate the isolation of fungi. Further selection of fungal colonies was carried out based on their morphological characteristics such as color and margin. These colonies were subsequently purified by streaking onto fresh PDB plates. Subsequent to the isolation process, we extracted fungal DNA utilizing the E.Z.N.A. DNA Kit (Omega Biotek Inc., Doraville, GA, USA). The ITS1F and ITS2 primers were employed to amplify the ITS1 regions, followed by Sanger sequencing. The obtained sequences were identified by comparing against the UNITE database. The isolated strains were preserved in a solution of 40% glycerol at a temperature of -80 °C and subcultured on PDB plates for subsequent analysis. MEGA X was employed for phylogenetic tree construction by the Neighbor-Joining method [50].

Plant growth–promotion assay

Single bacterial colonies were selected and inoculated into 1 mL of 1/2 Tryptic Soy Broth (TSB) liquid medium. The cultures were incubated at 28 °C with continuous agitation at 160 rpm on a shaker for a period of 48–72 h, ensuring that the logarithmic growth phase was achieved. Subsequently, 50 µl of the bacterial suspension was put onto 90 mm Petri dishes with 1/2 Murashige and Skoog (MS) agar medium. The sterile TSB served as a control. All fungal strains would be cultured on potato broth agar (PDA) at 25 °C until spores were produced. Spore suspensions (10 µL, 1×10^5 conidia/mL) were centrally inoculated on the agar plates, with sterile water as the control. Each strain was replicated three times.

We used 10% sodium hypochlorite (NaClO) for surface sterilization of tobacco seeds (cv. K326) for 10 min, which was rinsed three times using sterile water. After the sterilization seeds were germinated for 10 days on 1/2 MS agar medium, they were transferred onto the agar medium with the inoculated microbe colonies. Each agar plate accommodated five seedlings. The Petri dishes were put in a controlled growth chamber with normal conditions of 21 °C and a photoperiod of 16 h of darkness followed by 8 h of light for 10 days. The morphological indicators of the plants, including fresh weight, maximum leaf width, root length, plant height, and leaf number, were measured at the end of the experimental period.

Evaluation of tobacco growth promotion by volatiles produced by fungi

Tobacco seedlings were prepared as mentioned above. One seedling per well was placed on 1/2 MS agar amended with 3% sucrose in 6-well plates (Falcon, NJ, USA) with each well containing 4 mL of the medium. Two wells at one end of the plate were reserved for culturing F119 and F126; each well was incubated with conidia suspensions (2.5 µL, 1×10^6 conidia/mL). Plates were preformed three replicates for two fungi-incubated plates and control plate (with sterile water). The plates were sealed and aseptically maintained in a growth chamber set at 25 °C with a 14 h light and 10 h dark regime for 10 days. Similar morphological indicators of seedlings were collected and analyzed.

Whole genome sequencing of PGPR

Whole genome sequencing of B-9 and F126 was conducted using the Illumina MiSeq platform by Novogene Technology Co. Ltd (Tianjin, China). Sequencing quality was checked using FastQC (0.11.8). In total, 492,090 and 158,577 high-quality reads (Q > 35) were obtained for F126 and B-9, respectively. De novo assembly for high-quality scaffolds was performed using SPAdes v.3.9.0 [51]. The components of coding genes and functional annotation were performed using a range of databases including NCBI non-redundant (NR), SwissProt, COG, KEGG, and Gene Ontology (GO).

Statistical analysis

R (v4.2.0) tool were used for all statistical analysis in this study. The alpha-diversity, including Chao1 and Shannon indices, were performed using QIIME2. Multiple comparisons between alpha indices across different compartment niches, stages and treatments were assessed with the Kruskal–Wallis rank-sum test. Weighted UniFrac distance matrices were applied to determine beta-diversity, which were ordinated by onmetric multidimensional scaling (NMDS). To evaluate the relative contribution of different factors to community differences, the PERMANOVA (Permutational multivariate analyses of variance) test was conducted using "vegan" package. DESeq2 R package was used to identify differential expressed ASVs cross different treatments [52]. We performed LefSe (Linear discriminant analysis Effect Size) analysis between CNS-treated and control samples at the genus level. The genus, which had α less than 0.05 and an LDA score greater than 2 under one-against-all comparison mode, was referred as significant candidates between rhizosphere and soil. The significance of the growth index among different groups were evaluated using one-way analysis of variance (ANOVA) followed by the LSD test.

Results

The effects of CNS on plant growth

To assess the potential roles of CNS in regulating plant growth, we explored the effects of CNS in two concentrations (T1: 600 mg/L, T2: 1200 mg/L) (Fig. 1A, B). The application of CNS on tobacco vegetative and reproductive growth showed a dose-dependent manner (Fig. 1A, B). More specifically, T1 CNS concentration tended to improve the biomass accumulation of tobacco, exhibiting a remarkable 28.8% ± 8.5% increase in plant height. The application of T1 CNS concentration also resulted in an increase in the average number of leaves, increasing from 19.8 to 22.6. However, no differences in height and number of leaves were observed between T2 concentration CNS-treated and control plants (Fig. 1A). In addition, both concentrations had no significant effects on the internode length and leaf size (Figure S1 and Table S1). Furthermore, 25 days after treatment, tobacco plants under T1 CNS concentration exhibited a 1.6-fold increase in the flowering rate compared to control plants, whereas almost all plants treated with T2 CNS had not blossomed (flower rate: CK: 30%, T1: 78%, T2: 0%). The changes in biomass and flowering ratio for CNS-treated plants indicated that different CNS concentrations might tune up the duration of plant vegetative and reproductive growth.

Alteration of soil nutrients and enzyme activity upon exposure to CNS

Plants obtained water and nutrients from soil through root system for their growth, maintenance, and reproduction. Thus, the availability of various nutrients in soil directly affected the growth of plants. Principal Component Analysis (PCA) of the soil environmental factors could effectively distinguish different samples, with PC1 explaining 44.5% of the variance and PC2 explaining 18.5% (Fig. 1C). Upon exposure to CNS, the levels of soil nutrient elements showed significant changes, and various soil enzyme activities experienced a slight decrease (Figure S2). Under T1 CNS concentration treatment, the pH and available phosphorus content in the soil decreased, while the contents of total phosphorus, total nitrogen, nitrate nitrogen, and available phosphorus significantly increased compared to the CK group ($P < 0.05$). For T2 CNS concentration treatment, the available phosphorus, total phosphorus, and pH in the soil decreased, while the contents of total phosphorus and total nitrogen significantly increased compared to CK group ($P < 0.05$) (Figure S2). By measuring the activities of soil extracellular enzymes, we attempted to measure microbiome

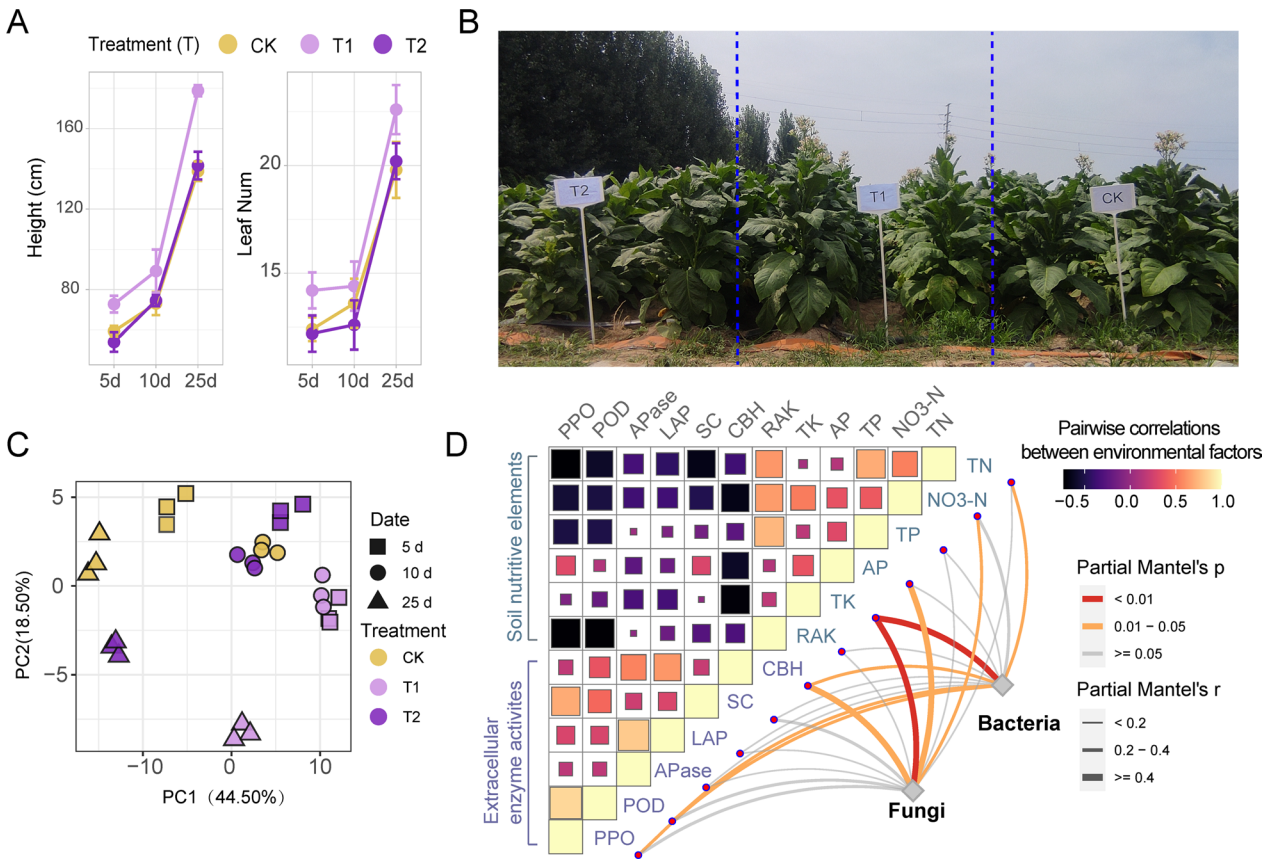

Fig. 1 Effects of CNS on the growth of tobacco in field experiment. **A** Effects of CNS on the plant height and leaf number of tobacco. **B** Comparison of tobacco morphology on 25 days after application of CNS at concentrations of 1200 mg/L CNS (T2), 600 mg/L CNS (T1) and water (CK) to the soil. **C** Principal component analysis (PCA) result of different samples using soil environmental factors. **D** Pairwise comparisons of environmental factors are shown, with a color gradient denoting Spearman's correlation coefficient. Taxonomic (based on bacterial and fungal ASVs) community composition was related to each environmental factor by Mantel tests. Edge width corresponds to Mantel's r statistic for the corresponding distance correlations, and edge color denotes the statistical significance based on 9,999 permutations

influence on soil. The activity of enzymes involved in cellobiohydrolase (CBH) and acid phosphatase (Apase) were found to be unaffected by CNS, whereas the activity of the other four enzymes (sucrase, leucine aminopeptidase, peroxidase and polyphenol oxidase) decreased significantly (Figure S2 and Table S2). Furthermore, correlation between microbial communities, and soil nutrients/enzyme activities demonstrated that total potassium content and CBH activity were significantly affected by microbial community composition (Fig. 1D and Table S3).

Effect of CNS on diversity and community assembly of microbiomes

To explore the influence of CNS on microbial community composition and diversity in different plant compartment niches (BS, RS, RP and R), sequencing of 16S rRNA and ITS gene amplicons were performed. T1 CNS concentration led to a slight but significant decrease in the alpha diversity of both bacteria and fungi ($P<0.05$), while T2 CNS concentration had no significant effect on both bacterial and fungal community diversity in terms of Chao1 richness index and Shannon diversity index ($P>0.05$, Fig. 2A). A similar trend was observed for different plant compartment niches, which showed a decreased richness and diversity pattern from bulk soil to rhizosphere, and finally to endosphere (Figure S3A and S3B).

Bray–Curtis dissimilarity was calculated to assess the differences in microbiome composition across different samples (Fig. 2B). The first two components explained about 50% variance of bacterial community across different samples, and samples could be clearly distinguished by compartment niches with the first component (41.59%). PCoA results also revealed significant differences between fungal communities across distinct compartment niches, while fungal samples could be much more distinguishable by developmental stages (Fig. 2B). Notably, CNS exhibited significant effects on

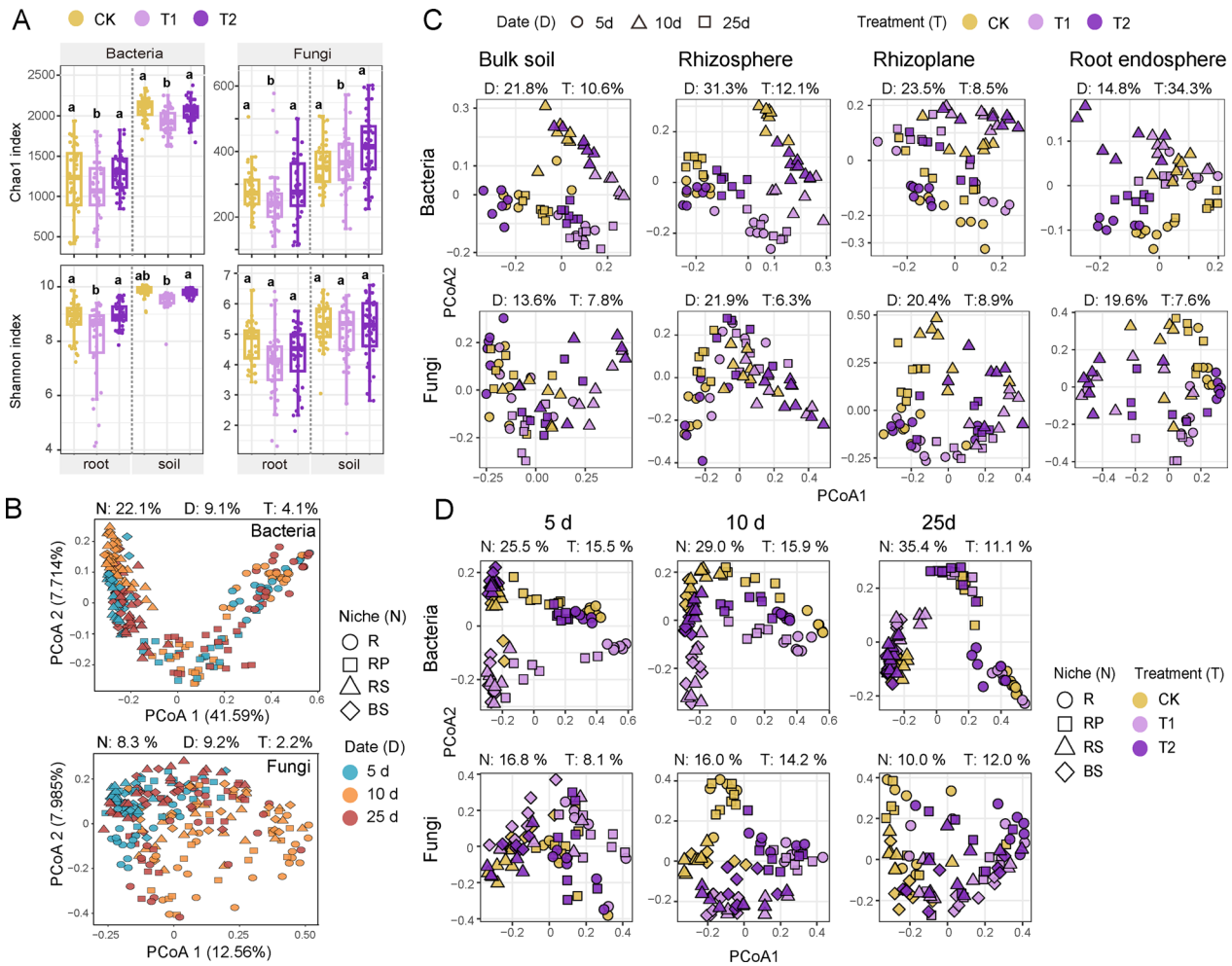

Fig. 2 CNS's effect on diversity of root-associated microbiomes. **A** Alpha-diversity of bacterial and fungal communities in root compartments (rhizoplane and root endosphere) and soils (rhizosphere and bulk soils) across three developmental stages after CNS treatment. ANOVA with an LSD test ($P < 0.05$) indicated statistically significant differences between different groups, denoting by different letters. **B** Nonmetric multidimensional scaling (NMDS) ordinations based on weighted UniFrac distance matrices depicting the distribution patterns of bacterial and fungal communities of all samples ($n = 216$). **C** Nonmetric multidimensional scaling (NMDS) ordinations based on weighted UniFrac distance matrices depicting the distribution patterns of bacterial and fungal communities in each compartment niche (for each niche, $n = 18$). **D** Nonmetric multidimensional scaling (NMDS) ordinations based on weighted UniFrac distance matrices depicting the distribution patterns of bacterial and fungal communities for each developmental stage (for each stage, $n = 24$). The relative contribution of different factors to community dissimilarity was tested with PERMANOVA. "T" represents the effect of the CNS treatment; "D" represents the effect of the developmental stage; "N" represents the effect of the compartment niche

microbial communities within different compartment niches (Fig. 2C). For the root endosphere, the influence of CNS on bacterial community structure was particularly prominent, accounting for 34.3% (Fig. 2C). In contrast, its impact on fungal community structure was relatively modest (6.3%-8.9%). During different developmental stages, a maximum relative contribution of CNS treatment (bacteria: 15.9%, fungi: 14.2%) was observed at 10d (Fig. 2D). In addition, CNS exhibited a great effect on both bacterial and fungal communities at the early stage, and then gradually recovered (Fig. 2D). Moreover, as shown by the Bray–Curtis distance, the lower concentration CNS might play greater roles in the assembly of both bacterial and fungal communities, being father away from the control samples (Fig. 2D).

Taxonomic classification revealed that CNS mildly tuned bacterial and fungal phyla (Fig. 3A, B). Tobacco root-associated bacterial communities were primarily composed of *Proteobacteria*, *Actinobacteriota*, *Acidobacteriota*, *Bacteroidota*, *Gemmatimonadota*, and *Firmicutes* (Fig. 3A). For fungal communities, *Ascomycota* and *Basidiomycota* phyla were dominated (Fig. 3B). With an

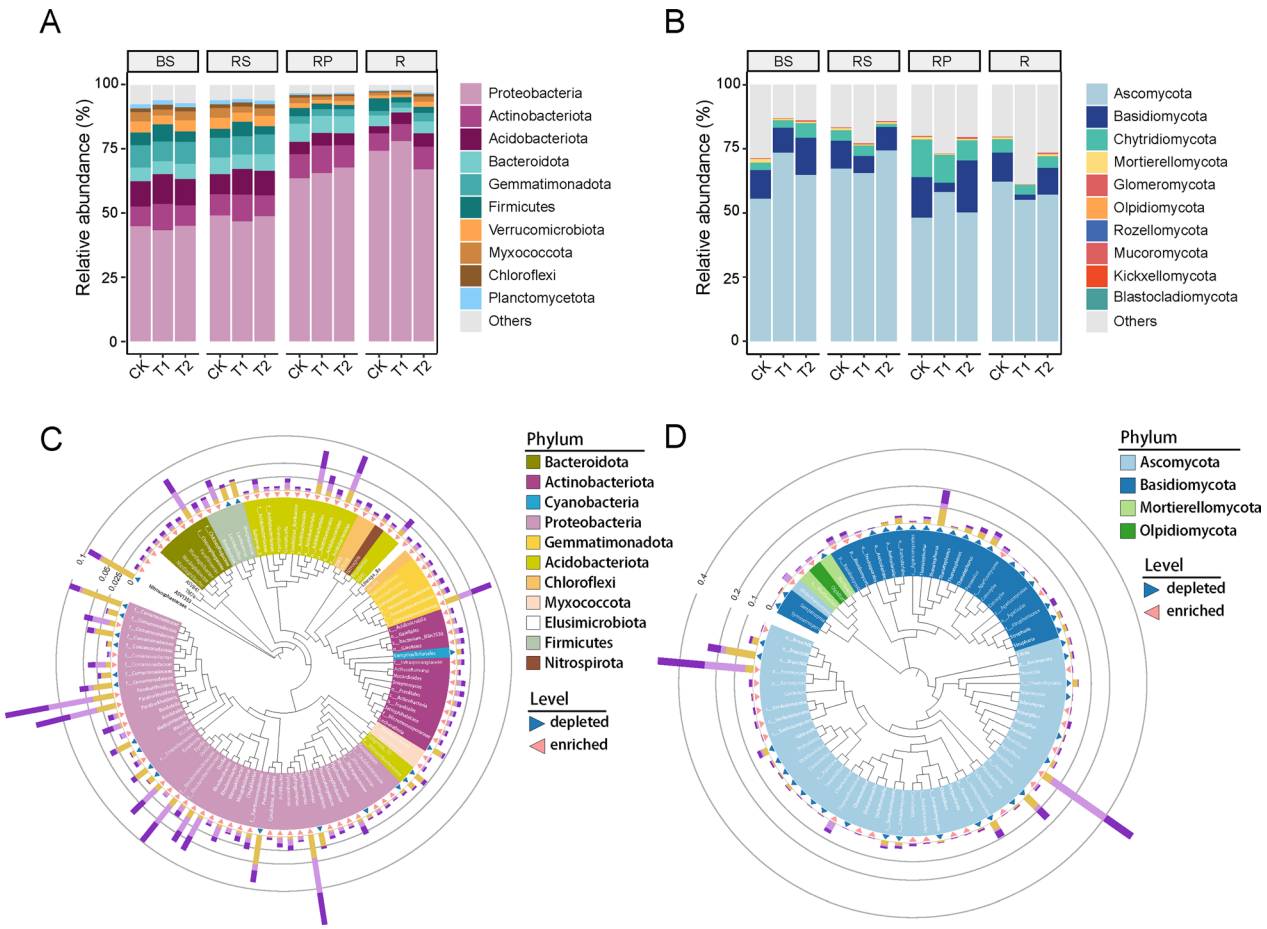

Fig. 3 Phylogenetic tree and taxonomic composition of root-associated microbiomes. Relative abundance of bacterial (**A**) and fungal (**B**) communities at the phylum level in the CNS-treated and control (CK) samples for four compartment niches: bulk soil (BS), rhizosphere soil (RS), rhizoplane soil (RP), and root endosphere (R); Phylogenetic tree of bacterial (**C**) and fungal (**D**) ASVs with differential abundances between CNS-treated and control samples. The red and blue triangles represent enrichment and depletion under CNS treatment, respectively. Inner circle colors represent different taxonomies at the order level. Bar graphs indicate the relative abundance in different groups

LDA score threshold of 2, enrichment/depletion pattern between CNS-treated and control samples was determined by LefSe analysis at the genus level. A total of 96 bacterial genera were identified to be enriched after CNS treatment (Figure S4A and Table S4). Among them, 49 were detected among both four compartments, such as *Sphingomonas*, *Dyella,* and *Rhodanobacter*. *Rhizorhapis* etc., were consistently depleted in the rhizosphere (Figure S5A). For fungal communities, 47 genera were enriched after CNS treatment (Figure S4B). Genera like *Penicillium*, *Myceliophthora*, and *Chrysanthotrichum* exhibited increased abundances across all compartment niches. In contrast, *Stropharia* and *Thanatephorus* showed consistent decreasing pattern across all compartment niches (Figure S5B).

Differential analysis of ASVs indicated that different genera exhibited various adaptabilities to CNS. A total of 1,148 distinct ASVs, encompassing 923 bacteria and 225 fungi, were identified as a response to CNS. A significant overrepresentation of the bacterial genera *Burkholderia*, *Sphingomonas*, *Lactobacillus*, *Streptomyces*, *Rhodanobacter*, and *Deylla* was observed in the rhizosphere under CNS treatment, while relative abundance of others, such as *Massilia* and *Pseudomonas* were decreased (Fig. 3C). Moreover, CNS exhibited a significant promoting effect for fungi. 91 and 125 fungal ASVs were enriched after T1 and T2 concentration CNS treatment, while 54 and 105 ASVs were decreased, respectively (Fig. 3D). CNS elevated the abundance of *Penicillium* and *Chrysanthotrichum*, and significantly inhibited the abundance of *Thanatephorus* and *Stropharia*. Notably, CNS treatment promoted the relative abundance of some potentially beneficial bacteria such as *Burkholderia*, *Sphingomonas*, and *Lactobacillus*, and some beneficial fungi such as *Penicillium*.

CNS elevates the complexity and stability of microbial interkingdom co-occurrence networks

To assess the impact of CNS on dynamics interaction among the microbiome, bacterial-fungal co-occurrence networks was constructed. CNS elevated complexity of microbial networks, with higher number of nodes and connecting edges after CNS treatment (CK: 268 nodes/559 edges, T1: 271 nodes/770 edges, T2: 258 nodes/582 edges) (Fig. 4A). Commonly, negative correlations reflected competition among microorganisms for resources within the microbial community. A higher number of negative correlations could enhance network stability by reducing community fluctuations in response to disturbances. Comparing with control samples, more negative interactions were observed for CNS treated samples (CK: 33.8%, T1: 53.8%, T2: 62.2%), indicating that competition and antagonism interactions among microorganisms were increased after CNS treatment.

To further characterize the compartment niche and CNS effect on microbe-microbe interactions, the co-occurrence dynamics were assessed along with the soil–plant niche (Figure S6). Complexity of network was gradually decreasing from soils (bulk soil and rhizosphere) to epiphytes (rhizoplane) and then to endophytes (root endosphere). Moreover, under lower concentration CNS treatment, the microbial networks of root endosphere showed decreased complexity and stability (with an average degree of 5.91 in CK and 3.93 in T1). This effect was a little recovered by higher concentration CNS treatment, with relative increasing average degree (4.45 in T2).

Within the network, bacteria and fungi might play distinct roles. In comparison to fungi, bacterial nodes in

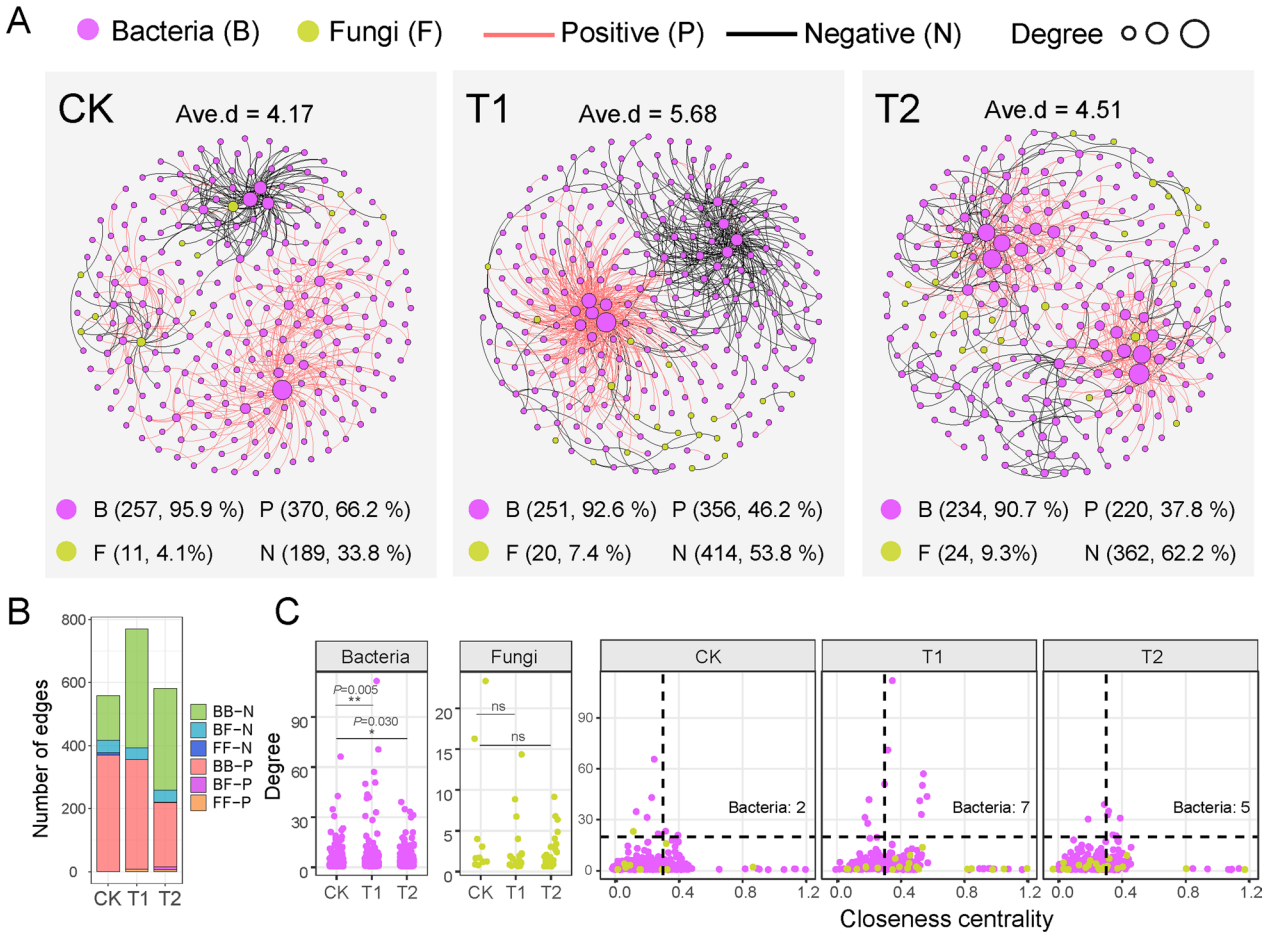

Fig. 4 Bacterial-fungal interkingdom co-occurrence networks. **A** Co-occurrence network analysis of full dataset (n = 216) showing microbial interkingdom network patterns for different groups. **B** Number of bacterial–bacterial (BB), bacterial–fungal (BF), and fungal–fungal (FF) correlations in the control (CK) and CNS-treated (T1 and T2) networks. "P" and "N" indicate positive and negative correlations, respectively. **C** Comparison of node-level topological features (degree and closeness centrality) between bacterial and fungal taxa at different groups. Asterisks indicate significant differences (nonparametric Wilcoxon rank test, $P \leq 0.05$) between the CNS-treated and control (CK) samples, and two asterisks indicate $P < 0.01$

the co-occurrence network held relative higher network degree (Fig. 4A). In addition, positive interactions among fungal community were elevated by CNS treatment (0% in CK, 18.2% in T1, and 13.6% in T2), while the reverse pattern was observed for bacterial community (77.3% in CK, 48.0% in T1, and 38.8% in T2) (Fig. 4B). These findings implied that fungi might adopt more collaborative roles under CNS treatment, potentially influencing plant growth. Hub microorganism for each network was defined using degrees (> 20) and closeness centrality (> 0.3). Our results revealed all the hub microorganisms for each network were bacteria (Fig. 4C and Table S5). Interestingly, *Sphingomonas* was one of hub microorganisms in the control network and T1 related network, and three hub microorganisms belonged to *Sphingomonas* (ASV2, ASV12, ASV18).

CNS induces shifts in abundances of plant growth-related genes in metagenomes

Metagenomic results demonstrated that the functional analysis (i.e. KEGG orthologs (KOs)) of CNS-treated root-samples significantly differed from the control samples ($R^2 = 44.3\%$, $P < 0.01$, Fig. 5A). There was an increased functional diversity for endophytic microbial communities under CNS treatment ($P < 0.01$) (Fig. 5B).

The differential abundance of various genes was inferred by performing LefSe analysis for four niches, and KOs associated with plant growth promotion were also predicted (Figure S7). The most enriched pathways under CNS treatment were nitrogen cycle related KOs (Fig. 5C). Consistently, the phosphate solubilization pathways were active under CNS treatment. Functional genes related to P transport system (e.g., *pstC* and *pstA*), organic P mineralization (e.g., *phnX* and *ugpQ*), and inorganic P solubilization (*PGD*), were enriched in root endosphere and rhizosphere under CNS treatment (Figure S7). CNS treatment also enriched more genes related to IAA biosynthesis pathways (e.g., *iaaM* and *trpB*) in the rhizosphere and rhizoplane, while they were depleted in the root endosphere (Figure S7). CNS also significantly promoted the gene abundance associated with sulfur metabolism (e.g., *cysK*, *cysA,* and *cysU*) and resistance to oxidative stress (*catB*, *gst,* and *fur*) in the bulk soil (Figure S7).

CNS-induced microbial consortium promotes plant growth

To investigate the function of specific ASVs enriched in CNS-treated root microbiota, we tried to isolate taxonomically diverse culturable bacterial and fungal from CNS-treated root samples. A total of 391 cultivable bacterial strains and 44 cultivable fungal strains were isolated, and identified by 16S rRNA and ITS rRNA gene sequencing (Fig. 6). Among these cultivable bacterial strains, 313 were corresponding to 225 ASVs from the 16S sequencing data, belonging to 57 different genera (Fig. 6A). The results indicated that the most abundant genus was *Pseudomonas*, with 11 isolates, accounting for 4.9%. It was followed by *Sphingobium* (6 isolates), *Rhizobium* (5 isolates), and *Burkholderia* (5 isolates). Among the culturable bacteria, 12 were significantly enriched ($P < 0.05$) after CNS treatment, including *Microbacterium*, *Variovorax*, *Bosea*, *Sphingopyxis*, *Stenotrophomonas*, and *Cupriavidus*, respectively, while 19 genera were significantly suppressed by CNS treatment ($P < 0.05$) (Fig. 6A). Among the 44 cultivable fungi, 7 were significantly enriched ($P < 0.05$) after CNS treatment, including *Wickerhamomyces*, *Stachybotrys*, *Myceliophthora*, *Talaromyces* (Fig. 6B).

To explore whether the isolated bacteria and fungi had an impact on plant growth, two significantly enriched fungi and twelve bacteria under CNS treatment were selected and inoculated with tobacco seedlings. Plate experiments demonstrated that the enriched bacteria were able to grow normally in the MS medium, with cloudiness observed. Among these testing strains, 6 bacteria belonging to *Microbacterium* (ASV-5, ASV-29), *Cupriavidus* (ASV-13), *Variovorax* (ASV-9) and *Sphingopyxis* (ASV-7 and ASV-25), and 2 fungi (F-119 and F-126), could effectively enhance the growth of tobacco seedlings (Fig. 7A, B). During 15-day inoculation period, notable increasing in fresh weight, leaf number, and leaf size were observed for tobacco seedling in comparison to the control group (Figure S8). Among these bacteria, ASV-9, identified as the *Variovorax* genus, showed the best growth-promoting effect. After inoculation, the fresh weight increased by 159.71% compared with the control, with an average maximum leaf width of 1.48 cm (1.65 times than control) and an average of 3.73 true leaves (3.21 times than control). Two fungi, especially F-119, after co-cultivation with plants, led to twice fresh weight, higher leaf numbers, and wider leaves than the control ($P < 0.05$, Figure S8). Hence, it could be inferred that CNS treatment possibly achieved its growth-promoting effects by influencing the abundance of these beneficial strains.

CNS-enriched fungi enhances plant growth by plant growth promotion hormones and volatile compounds

F-119 was identified as fungus within the *Cladosporium* genus through ITS rRNA sequencing, showing a maximum similarity of 98% with the *Cladosporium herbarium* (Fig. 7C). F-126 belonged to the *Talaromyces* genus, with a maximum similarity of 97.93% to the *Talaromyces funiculosus* (Fig. 7C). Next, we attempted to explore how these two fungi induce growth-promoting effects. Given their capacity to promote growth without direct physical

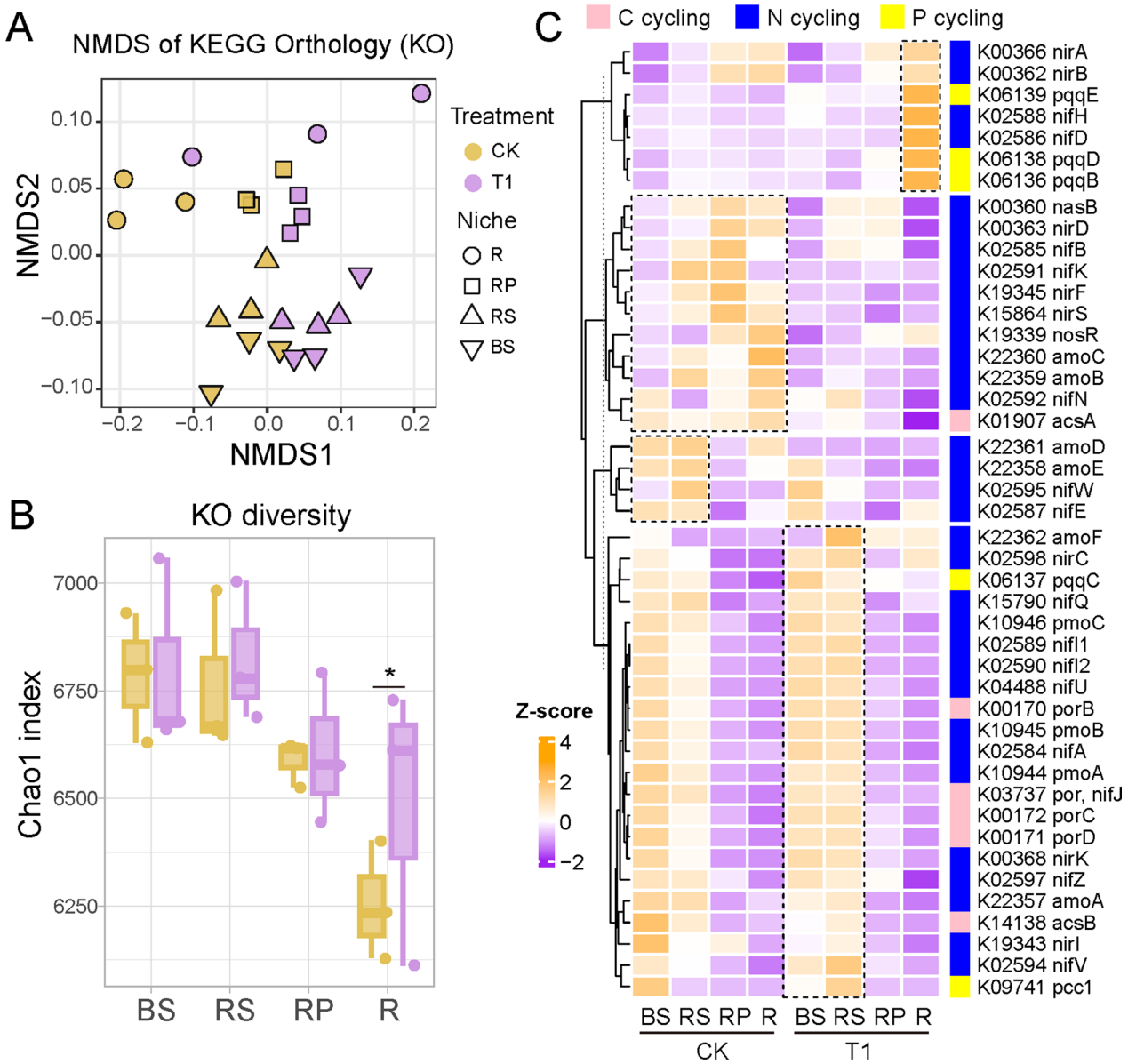

Fig. 5 Functional profiles of tobacco root microbiomes. **A** Nonmetric multidimensional scaling (NMDS) ordination analysis based on Bray–Curtis distance matrices of the KEGG ontology annotations. **B** Boxplot of the functional diversity of microbiomes in four compartment niches. Asterisks above the boxes indicate a significant difference ($P < 0.05$). **C** Heatmap exhibiting the relative abundance of functional genes associated with plant growth–promotion functions. All genes associated with plant growth–promotion functions are listed in Table S7. The four compartment niches are bulk soils (BS), rhizosphere (RS), rhizoplane (RP), and root endosphere (R)

contact with tobacco seedlings, we hypothesize that their effects may be mediated through the release of secretions or organic volatile compounds (VOCs). As shown in Fig. 7D, F-126 and F-119 could still facilitate the accumulation of tobacco biomass even when the seedlings were grown physically separated from these two strains in an airtight chamber. The VOCs released by these two fungi strains showed significant enhancement in both the aboveground and underground parts of tobacco seedlings ($P < 0.05$, Fig. 7E). This observation suggested that their growth-promoting effects might be partially mediated by VOCs.

Indole-3-acetic acid (IAA) was a plant hormone that regulated plant root growth by stimulating the proliferation and elongation of root cells. The *trpABC*, *trpE*, and *amiE* involved in regulating the tryptophan-dependent IAA synthesis pathway were present in the genomes of *Talaromyces* sp. strain F-126. Moreover, there were genes

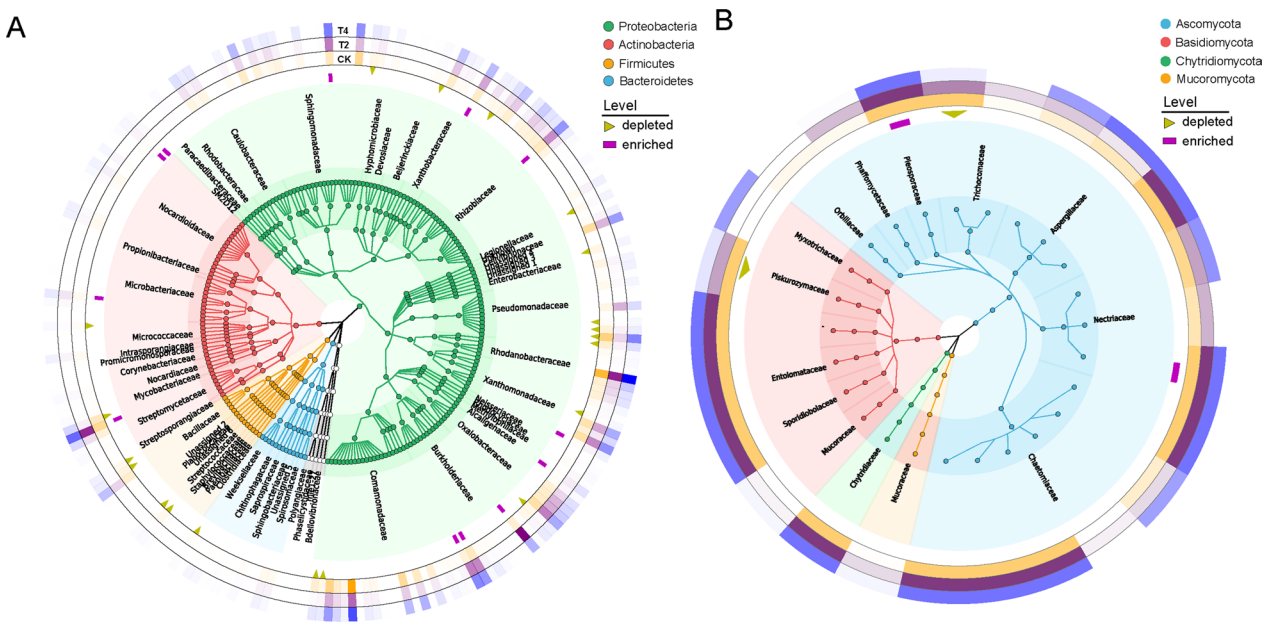

Fig. 6 Phylogenetic tree of isolated culturable bacterial (**A**) and fungal (**B**) from tobacco root-associated samples. The tree represents the bacteria/fungal ASVs reproducibly detected in the roots of tobacco (with relative abundance greater than 0.01%). The inner ring indicates the taxonomic distribution at order level; The middle ring with purple squares and yellow-green triangles represents enriched or depleted ASVs under CNS treatment. The relative abundances in different groups are shown in the outermost ring of the heatmap

encoding ACC deaminase, which could break down the precursor (ACC) of ethylene in F-126 genome, thereby reducing the levels of ethylene, and in turn promoted root elongation and branching (Figure S9).

Discussion

CNS strongly influences the assembly of root-associated microbiomes

Similar with previously studies, incorporating nanomaterials (NMs) into the soil would affect rhizospheric microbes, and enhance plant roots and crop growth, which offered novel strategies for optimizing agricultural practices and addressing the challenges of sustainable food production in the future. Previous research had demonstrated that relative concentrations of CNS could enhance plant growth in controlled environments, such as suspension cultures, hydroponics, and laboratory pot experiments [32]. For instance, CNS promoted the absorption of potassium ions by tobacco roots in hydroponic [53]. Despite the promising capacity of CNS, the cascading effects of CNS, via the roots, on plant physiology and plant–microbiota interaction remained elusive. Here, we tried to use high throughput sequencing analysis and culture collection to investigate the effects of CNS on plant growth and root-associated microbiota in field experiments. Overall, our findings revealed distinct differences in the composition, microbiome interactions, and metabolic capacity of root-associated microbiome between CNS-treated plants and control plants. Further, multiple microbial attributes revealed that microbiomes in the endosphere compartment were more sensitive to CNS than soil microbiomes, such as alpha-diversity, microbiome composition, and interkingdom co-occurrence networks. Plants exposed to CNS reshaped root-associated microbiome with high abundance of beneficial bacteria, forming a relative stable network enriched with beneficial hub microorganisms that favored plant growth. Based on cultivated bacteria and fungi, we found that CNS treatment led to the recruitment of specific beneficial microbiota, such as *Sphingomonas, Variovorax*, and *Burkholderia*, which in turn enhanced plant growth. In summary, these discoveries provided valuable insights into the recruitment of specific root-associated microorganisms in plants exposed to CNS. In this study, CNS was introduced into the plant through root irrigation. However, it was worth noting that alternative application methods might need further investigation. For instance, the delivery of CNS via spray onto leaf surfaces might represent a promising avenue for future research, which might reduce soil fixation and ensure more efficient absorption by the plant. One recent study has demonstrated that the

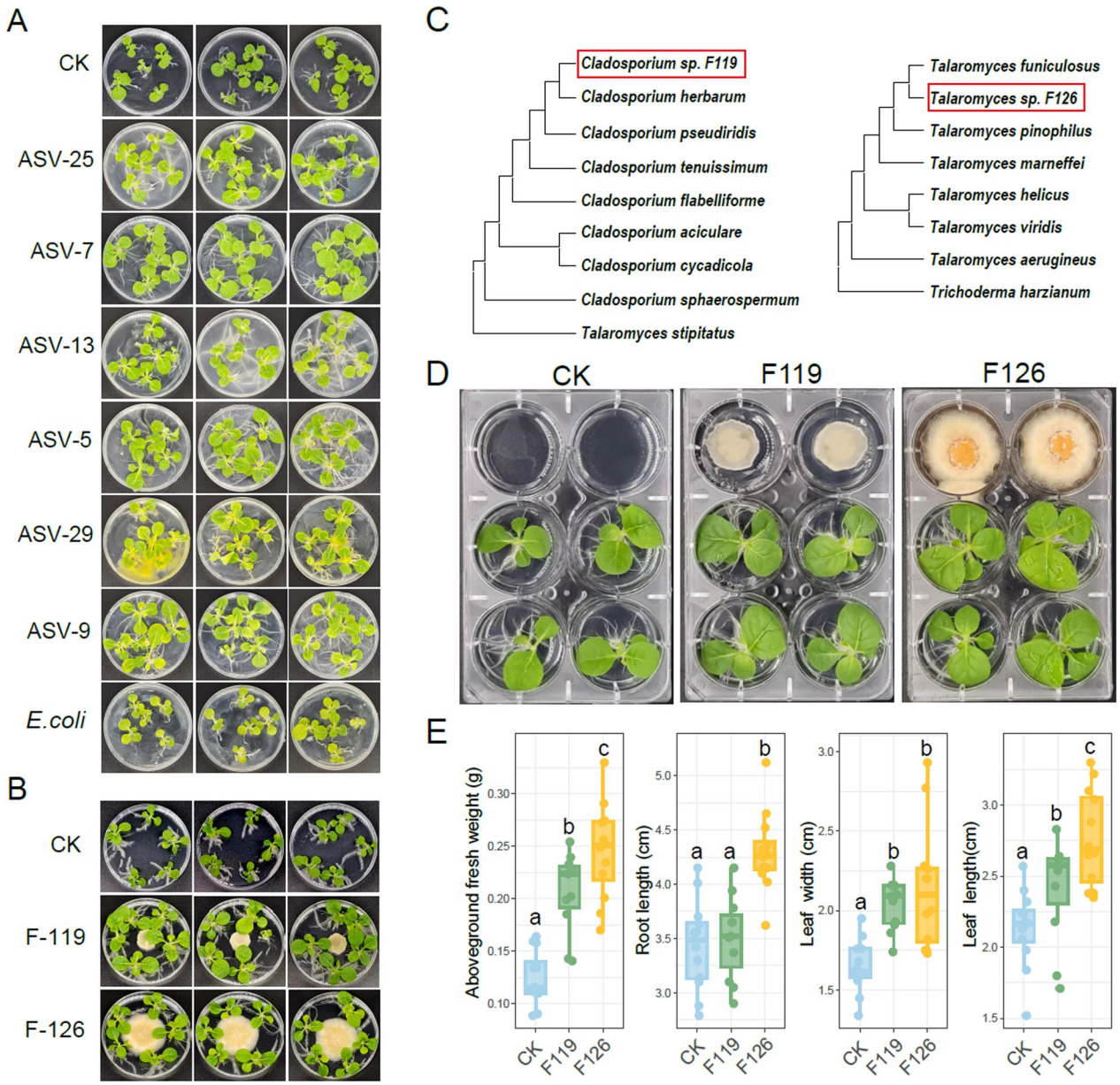

Fig. 7 The growth promotion effect of CNS enriched isolations. **A** Phenotype of tobacco seedlings after inoculation with CNS-enriched bacteria on MS plates. Distilled water was used as the negative control, and *Escherichia coli* served as the positive control. **B** Phenotype of tobacco seedlings after inoculation with CNS-enriched fungi on MS plates. **C** Phylogenetic analysis of two isolated Fungi. Neighbor-joining trees were constructed using partial ITS gene sequences of F119 and F126 and their close relatives. *Trichoderma harzianum* was used as outgroup for rooting the tree. **D** Phenotype of tobacco seedlings after inoculation with two fungi F119 and F126 in 6-well culture plates without physical contact. **E** Box plots showing growth parameters of tobacco seedlings exposure to volatile compounds of F119 and F126 for 10 days. ANOVA with an LSD test ($P < 0.05$) indicated statistically significant differences denoted by different letters for each assessed parameter

foliar application of carbon nanosol at concentration of 40–70 μg/mL could also promote the growth of tobacco seedlings [54].

The dose-dependent and phase-dependent effects of CNS on the microbiome composition

Numerous studies had highlighted the various impact of ENMs on plant growth, yield, and quality, pointing out various factors might affect their pivotal roles, such as type, concentration, size, application mode, exposure

duration, and plant species [55, 56]. Although great progress had been derived in engineering the plant-associated microbial communities using ENMs, many of these studies only focused on short-term investigations or the effects of a single nanomaterial concentration within controlled laboratory conditions, like potted plants in the greenhouse. In contrast, our study aimed to explore various concentrations of CNS and their dynamic interactions with the microbial community under natural field conditions. Our findings revealed a dose-dependent and time-dependent influence of CNS on both plant performance and the associated soil microbiome. 25 days after CNS treatment, microbial communities still exhibited significant differences, suggesting that changes in microbial community composition resulting from CNS might not be transient. The impacts of CNS on microbiota were observed more pronounced at 10 days, and over time, the disturbance caused by CNS gradually recovered (Fig. 2D).

We also observed the remarkable dose-dependent influence of CNS on plant growth and development (Fig. 1C). Low and high-concentration CNS caused earlier or later flowering times, respectively. Notably, lower concentrations of CNS led to earlier flowering by shortening the vegetative development phase, consistent with previous studies [57, 58]. These dose-dependent responses were likely due to intricate mechanisms encompassing direct toxicity, dynamics in microbial community, and resource competition among microorganisms [59]. High ENM concentrations have been shown to induce cellular stress [60], disrupt metabolism [61], and suppressed growth for both plants and microorganisms [62]. Moreover, elevated ENM levels could alter microbial community composition of different compartment niches, potentially fostering resource competition among microorganisms. For example, the structure and metabolism of the endophytic bacterial community in roots underwent remarkable changes under CNS treatment. These complex interactions, along with stress-induced responses and metabolic changes, might collectively contribute to the dose-dependent effects of ENM on plant-microorganism interactions. In summary, our research indicated the importance of ENM concentration and exposure duration when assessing their impact on plants and associated microbiomes. These insights expanded our understanding of the intricate interplay between ENMs and biological systems. In future practical applications, our results indicated that CNS could be strategically applied to enhance plant growth and improve soil health, potentially reducing the need of fertilizers and pesticides. This offered valuable insights for developing sustainable agricultural practices, where careful management of ENM application could lead to more resilient crops and healthier ecosystems.

The alteration in ecological functions of microbiome communities under CNS addition

Soil microbiome could play important roles in determining soil environmental properties including mineralization, pH, and nutrient availability [63]. The surface of ENMs could affect their hydrophobicity, and soil environments, provoking mobilization and nutrient mineralization and through rhizospheric microorganisms [64]. Moreover, root-associated microbiota could produce abundant bioactive secondary metabolites, including phytohormones and siderophores. We applied metagenome to explore relevant functions for rhizosphere community associated with plant growth from both the soil and root, aiming to establish a link between these functions and the microbiome composition within tobacco roots. In summary, the relative abundances of some specific genes were much higher among the CNS-treated samples compared to the control, which might account for the observed enhancement in plant growth (Fig. 5C and S7). In our study, the abundance of genes related to the sulfur cycle pathways, nitrogen metabolism, and phosphate solubilization within the tobacco rhizosphere and endosphere were increased under CNS treatment. Similar to our findings, other studies have also shown that microorganisms could promote plant growth by improving the availability of nutrients, thereby enhancing the uptake of plants. Recent rhizospheres functional studies of *Arabidopsis* and soybean have revealed the roles of iron acquisition and mineral nutrient metabolism for plant growth [65, 66]. Insufficient available nitrogen and soluble phosphate could inhibit plant growth [67]. Another noteworthy enhancement was observed in rhizosphere functions involved in the production of plant growth regulators, including IAA, 2,3-butanediol, and acetoin, all of which could promote plant growth [68]. In our study, the enhanced plant growth-promoting effect, coupled with the differences among various microbial communities, suggested that the microbial community played a crucial mediating role between soil conditions, CNS application, and plant performance. Additionally, the observed increase in soil phosphorus availability, together with the elevated abundances in genes related to the solubilization of phosphorus, further supported the role of the root-associated microbial community in linking CNS application with soil quality improvement.

CNS-enriched microbial strains and their effects on plant growth

Our microbiome analysis unveiled a notable enrichment of plant-beneficial microorganisms following CNS treatment, implying an increased colonization of potential plant growth-promoting microorganisms. Furthermore, we isolated the bacteria and fungi enriched under CNS

treatment, and confirmed their plant growth-promoting effects. These findings highlighted the potential of CNS applied to plant roots for targeted and precise manipulation of microbiomes. Further research was needed to explore the potential advantages of utilizing complex synthetic microbial communities, comprising a mix of plant beneficial microbes. These communities might offer synergistic benefits that enhanced plant growth, resilience to environmental stressors, and nutrient uptake in ways that might be difficult or impossible to single-strain inoculants [69]. The study of such interactions between different strains could deepen our understanding of the optimal conditions for using microbial consortia in sustainable agriculture.

Except promoting plant growth by the production of phytohormones, these beneficial microbiomes could also accelerate nutrient availability and suppress disease. Commonly, these beneficial microbes could strengthen the nutrient status of plants by P solubilization or N fixation, enhancing surface area of roots, and increasing the available nutrients in the rhizosphere [70]. Many previous studies have demonstrated that *Variovorax sp*. was regarded as potential plant growth-promoting bacteria for many plants [71]. Genomic analysis of the *Variovorax* sp. B9, a prominent PGPR enriched under CNS treatment, revealed the presence of functional genes associated with IAA production, ACC deaminase activity, as well as phosphorus solubilization, and nitrogen fixation capabilities (Figure S10).

It was noteworthy that several studies have reported fungi and bacteria might influence plant growth through VOC production [72]. These VOCs were often composed of simple hydrocarbons, alcohols, esters, and other small molecules that could directly impact plant physiology. For instance, 2,3-butanediol and acetoin have demonstrated a strong capacity to promote plant growth and trigger induced resistance against fungal pathogens, exhibiting antimicrobial activity [73]. Current research suggested that VOCs functioned as plant growth boosters by activating various signaling pathways, often in correlation with plant growth hormones [74]. These VOCs were produced through specific metabolic pathways in microbe, as secondary metabolites during their interactions with plants. In particular, *Trichoderma* spp. had the capability to produce these volatile secondary metabolites, which played important function in the interaction between *Trichoderma* and plants [75]. Additionally, our partitioned plate experiments indicated that two PGPR fungi might exert their growth-promoting effects through the production of VOCs (Fig. 7D and 7E). However, further investigations using mutant strains of these VOCs were needed to identify specific compounds responsible for the plant–microbe interactions. It would be useful to identify suitable VOCs, which would provide promising commercial products in crop grown.

Conclusions

This work extended previous findings on the impact of CNS addition on the tobacco root community, as well as the alterations in plant growth and soil properties. Our results revealed that CNS treatment significantly influenced plant growth and soil nutrient availability in a dose-dependent manner. Specifically, to some extent, the relative lower concentration (600 mg/L) of CNS shortened vegetative growth duration and phosphorus availability. A substantial shift in the root-associated microbiome assembly in CNS-treated plants compared to control plants was observed. Moreover, the diversity and structure of fungal and bacterial communities exhibited phase and dose-dependent responses to CNS. Remarkably, the microbial networks in CNS-treated plants exhibited greater complexity, increased connectivity, and the presence of more hub microorganisms than those in control plants. Our analysis revealed that some potential plant-beneficial microorganisms were highly enriched under CNS treatment, including *Sphingomonas*, *Burkholderia*, *Penicillium*, *Myceliophthora*, and *Talaromyces*. Furthermore, 391 culturable bacteria and 44 culturable fungi were isolated from soil and root samples. Finally, 6 bacterial and 2 fungi were validated to have microbial-mediated growth effects on tobacco, and these two fungi performed their functions by volatile organic compounds (VOCs). Our investigation broadened the understanding of CNS impacts on plant–microbe interactions and underscored the promising practice of utilizing nanomaterials to modulate microbiome.

Supplementary Information

The online version contains supplementary material available at https://doi.org/10.1186/s12951-024-02971-x.

Supplementary material 1.

Supplementary material 2.

Acknowledgements

This work was supported by the Natural Science Foundation of HeNan (232300420220); Zhengzhou Tobacco Research Institute [CNTC: 110202201001(JY-01), 110202202038], chief scientist innovation project of State Tobacco Monopoly Administration/China National Tobacco Corporation (902023CK0880), Beijing Life Science Academy [BLSA: 2023000CC0110].

Author contributions

JJJ and PJC conceived and designed the experiments. LTC, PL, HS and JMT performed bioinformatics data analysis. LTC, JFZ, ZCQ and HL did microbial related experiments. LTC, WH, WJM, WZ, NL, PJC and JJJ wrote the manuscript and all authors read and approved the final version.

Data availability

The raw sequence data reported in this paper have been deposited in the Genome Sequence Archive in BIG Data Center, Beijing Institute of Genomics

(BIG), Chinese Academy of Sciences, under accession numbers CRA013578 (Raw 16S rRNA and ITS amplicon sequences), CRA013566 (metagenome sequences), and CRA013567 (genome sequence), which can be publicly accessible at http://bigd.big.ac.cn/gsa.

Declarations

Competing interests

The authors declare that they have no known competing financial interests or personal relationships that could have appeared to influence the work reported in this paper.

Author details

[1]Beijing Life Science Academy, Beijing 102200, China. [2]China Tobacco Gene Research Center, Zhengzhou Tobacco Research Institute of CNTC, Zhengzhou 450001, China. [3]Key Laboratory of Ecological Environment and Tobacco Quality, Zhengzhou Tobacco Research Institute of CNTC, Zhengzhou 450001, China. [4]Henan Provincial Tobacco Company, Zhengzhou 450001, China. [5]Fujian Tobacco Industry Co., Ltd, Xiamen 361001, China. [6]China National Tobacco Quality Supervision & Test Center, Zhengzhou 450001, China. [7]School of Agricultural Sciences, Zhengzhou University, Zhengzhou 450001, China.

Received: 30 July 2024 Accepted: 3 November 2024
Published online: 09 November 2024

References

1. Arif I, Batool M, Schenk PM. Plant microbiome engineering: expected benefits for improved crop growth and resilience. Trends Biotechnol. 2020;38(12):1385–96.
2. Bhattacharyya PNJD. Plant growth-promoting rhizobacteria (PGPR): emergence in agriculture. World J Microbiol iotechnol. 2012;28(4):1327–50.
3. Yazdani M, Bahmanyar MA, Pirdashti H, Esmaili MA. Effect of phosphate solubilization microorganisms (PSM) and plant growth promoting rhizobacteria (PGPR) on yield and yield components of corn (Zea mays L.). World Acad Sci Eng Technol. 2009;49(1):90–2.
4. Lucas Garcia J, Probanza A, Ramos B, Barriuso J, Gutierrez Manero F. Effects of inoculation with plant growth promoting rhizobacteria (PGPRs) and Sinorhizobium fredii on biological nitrogen fixation, nodulation and growth of Glycine max cv. Osumi. Plant Soil. 2004;267:143–53.
5. Ipek M, Aras S, Arıkan Ş, Eşitken A, Pırlak L, Dönmez MF, Turan M. Root plant growth promoting rhizobacteria inoculations increase ferric chelate reductase (FC-R) activity and Fe nutrition in pear under calcareous soil conditions. Sci Hortic. 2017;219:144–51.
6. Bal HB, Nayak L, Das S, Adhya TK. Isolation of ACC deaminase producing PGPR from rice rhizosphere and evaluating their plant growth promoting activity under salt stress. Plant Soil. 2013;366:93–105.
7. Goswami D, Thakker JN, Dhandhukia PC. Portraying mechanics of plant growth promoting rhizobacteria (PGPR): a review. Cogent Food Agric. 2016;2(1):1127500.
8. Della Mónica IFWVA, Stefanoni Rubio PJ, Vaca-Paulín R, Yañez-Ocampo G. Exploring plant growth-promoting rhizobacteria as stress alleviators: a methodological insight. Arch Microbiol. 2022;204(6):316.
9. Ahmed T, Noman M, Gardea-Torresdey JL, White JC, Li B. Dynamic interplay between nano-enabled agrochemicals and the plant-associated microbiome. Trends Plant Sci. 2023;16:1310.
10. An C, Sun C, Li N, Huang B, Jiang J, Shen Y, Wang C, Zhao X, Cui B, Wang C. Nanomaterials and nanotechnology for the delivery of agrochemicals: strategies towards sustainable agriculture. J Nanobiotechnol. 2022;20(1):1–19.
11. Hussain M, Shakoor N, Adeel M, Ahmad MA, Zhou H, Zhang Z, Xu M, Rui Y, White JC. Nano-enabled plant microbiome engineering for disease resistance. Nano Today. 2023;48: 101752.
12. Liu Y, Cao X, Yue L, Wang C, Tao M, Wang Z, Xing B. Foliar-applied cerium oxide nanomaterials improve maize yield under salinity stress: reactive oxygen species homeostasis and rhizobacteria regulation. Environ Pollut. 2022;299: 118900.
13. Ahmed T, Noman M, Jiang H, Shahid M, Ma C, Wu Z, Nazir MM, Ali MA, White JC, Chen J. Bioengineered chitosan-iron nanocomposite controls bacterial leaf blight disease by modulating plant defense response and nutritional status of rice (Oryza sativa L.). Nano Today. 2022;45:101547.
14. Wang C, Yue L, Cheng B, Chen F, Zhao X, Wang Z, Xing B. Mechanisms of growth-promotion and Se-enrichment in Brassica chinensis L. by selenium nanomaterials: beneficial rhizosphere microorganisms, nutrient availability, and photosynthesis. Environ Sci Nano. 2022;9(1):302–12.
15. Rashid MI, Shah GA, Sadiq M, Amin Nu, Ali AM, Ondrasek G, Shahzad K. Nanobiochar and copper oxide nanoparticles mixture synergistically increases soil nutrient availability and improves wheat production. Plants. 2023;12(6):1312.
16. Afzal S, Singh NK. Effect of zinc and iron oxide nanoparticles on plant physiology, seed quality and microbial community structure in a rice-soil-microbial ecosystem. Environ Pollut. 2022;314: 120224.
17. Zhao L, Chen S, Tan X, Yan X, Zhang W, Huang Y, Ji R, White JC. Environmental implications of MoS2 nanosheets on rice and associated soil microbial communities. Chemosphere. 2022;291: 133004.
18. Khan ST. Interaction of engineered nanomaterials with soil microbiome and plants: their impact on plant and soil health. Sustain Agric Rev. 2020;41:181–99.
19. Wang C, Yue L, Cheng B, Chen F, Zhao X, Wang Z, Xing B. Mechanisms of growth-promotion and Se-enrichment in Brassica chinensis L. by selenium nanomaterials: beneficial rhizosphere microorganisms, nutrient availability, and photosynthesis. Environ Sci Nano. 2022;9(1):302–12.
20. Zhang W, Jia X, Chen S, Wang J, Ji R, Zhao L. Response of soil microbial communities to engineered nanomaterials in presence of maize (Zea mays L.) plants. Environ Pollut. 2020;267:115608.
21. Lewis RW, Bertsch PM, McNear DH. Nanotoxicity of engineered nanomaterials (ENMs) to environmentally relevant beneficial soil bacteria–a critical review. Nanotoxicology. 2019;13(3):392–428.
22. Khanna K, Kohli SK, Handa N, Kaur H, Ohri P, Bhardwaj R, Yousaf B, Rinklebe J, Ahmad P. Enthralling the impact of engineered nanoparticles on soil microbiome: a concentric approach towards environmental risks and cogitation. Ecotoxicol Environ Saf. 2021;222: 112459.
23. Rodrigues ES, Montanha GS, de Almeida E, Fantucci H, Santos RM, de Carvalho HW. Effect of nano cerium oxide on soybean (Glycine max L. Merrill) crop exposed to environmentally relevant concentrations. Chemosphere. 2021;273:128492.
24. Cao Z, Stowers C, Rossi L, Zhang W, Lombardini L, Ma X. Physiological effects of cerium oxide nanoparticles on the photosynthesis and water use efficiency of soybean (Glycine max (L.) Merr). Environ Sci Nano. 2017;4(5):1086–94.
25. Zhao F, Xin X, Cao Y, Su D, Ji P, Zhu Z, He Z. Use of carbon nanoparticles to improve soil fertility, crop growth and nutrient uptake by corn (Zea mays L.). Nanomaterials. 2021;11(10):2717.
26. Wang H, Zhang M, Song Y, Li H, Huang H, Shao M, Liu Y, Kang Z. Carbon dots promote the growth and photosynthesis of mung bean sprouts. Carbon. 2018;136:94–102.
27. Rahmani N, Radjabian T, Soltani BM. Impacts of foliar exposure to multi-walled carbon nanotubes on physiological and molecular traits of Salvia verticillata L., as a medicinal plant. Plant Physiol Biochem. 2020;150:27–38.
28. Chung H, Kim MJ, Ko K, Kim JH, Kwon H-a, Hong I, Park N, Lee S-W, Kim W. Effects of graphene oxides on soil enzyme activity and microbial biomass. Sci Total Environ. 2015;514:307–13.
29. Asadishad B, Chahal S, Akbari A, Cianciarelli V, Azodi M, Ghoshal S, Tufenkji N. Amendment of agricultural soil with metal nanoparticles: effects on soil enzyme activity and microbial community composition. Environ Sci Technol. 2018;52(4):1908–18.
30. Pietroiusti A, Magrini A, Campagnolo L. New frontiers in nanotoxicology: gut microbiota/microbiome-mediated effects of engineered nanomaterials. Toxicol Appl Pharmacol. 2016;299:90–5.
31. Ge Y, Schimel JP, Holden PA. Identification of soil bacteria susceptible to TiO2 and ZnO nanoparticles. Appl Environ Microbiol. 2012;78(18):6749–58.
32. Chen LYJ, Li X, Liang T, Nie C, Xie F, Liu K, Peng X, Xie J. Carbon nanoparticles enhance potassium uptake via upregulating potassium channel expression and imitating biological ion channels in BY-2 cells. J Nanobiotechnology. 2020;18:21.

33. Yang JLT, Li HJ, Yin QS, Zhang YL, Zhou HP, Zhang SX. Effects of nano-carbon sol on physiological characteristics of root system and potassium absorption of flue-cured tobacco. Yancao Keji. 2015;48(1):7–11.
34. Wang C, Hua Y, Liang T, Guo Y, Wang L, Zheng X, Liu P, Zheng Q, Kang Z, Xu Y. Integrated analyses of ionomics, phytohormone profiles, transcriptomics, and metabolomics reveal a pivotal role of carbon-nano sol in promoting the growth of tobacco plants. BMC Plant Biol. 2024;24(1):473.
35. Li D, Li T, Yang X, Wang H, Chu J, Dong H, Lu P, Tao J, Cao P, Jin J. Carbon nanosol promotes plant growth and broad-spectrum resistance. Environ Res. 2024;251: 118635.
36. Cheng L, Tao J, Qu Z, Lu P, Liang T, Meng L, Zhang W, Liu N, Zhang J, Cao P. Carbon nanosol-induced assemblage of a plant-beneficial microbiome consortium. J Nanobiotechnol. 2023;21(1):436.
37. Chen LWH, Li X, Nie C, Liang T, Xie F. Highly hydrophilic carbon nanoparticles: uptake mechanism by mammalian and plant cells. RSC Adv. 2018;8:35246–56.
38. Cui A-L, Feng G-X, Zhao Y-F, Kou H-Z, Li H, Zhu G-H, Hwang H-S, Oh H-C, Kwon Y-J, Lee D-C. Synthesis and separation of mellitic acid and graphite oxide colloid through electrochemical oxidation of graphite in deionized water. Electrochem commun. 2009;11(2):409–12.
39. Xiong C, Zhu YG, Wang JT, Singh B, Han LL, Shen JP, Li PP, Wang GB, Wu CF, Ge AH. Host selection shapes crop microbiome assembly and network complexity. New Phytol. 2021;229(2):1091–104.
40. Bell CW, Fricks BE, Rocca JD, Steinweg JM, McMahon SK, Wallenstein MD. High-throughput fluorometric measurement of potential soil extracellular enzyme activities. J Vis Exp. 2013;81: e50961.
41. Quast CPE, Yilmaz P, Gerken J, Schweer T, Yarza P, Peplies J, Glöckner FO. The SILVA ribosomal RNA gene database project: improved data processing and web-based tools. Nucleic Acids Res. 2013;41(Database issue):D590-596.
42. Nilsson RHLK, Taylor AFS, Bengtsson-Palme J, Jeppesen TS, Schigel D, Kennedy P, Picard K, Glöckner FO, Tedersoo L, Saar I, Kõljalg U, Abarenkov K. The UNITE database for molecular identification of fungi: handling dark taxa and parallel taxonomic classifications. Nucleic Acids Res. 2019;8(D1):D259–64.
43. Nurk SMD, Korobeynikov A, Pevzner PA. metaSPAdes: a new versatile metagenomic assembler. Genome Res. 2017;5:824–34.
44. Huerta-Cepas J, Szklarczyk D, Heller D, Hernández-Plaza A, Forslund SK, Cook H, Mende DR, Letunic I, Rattei T, Jensen LJ. eggNOG 5.0: a hierarchical, functionally and phylogenetically annotated orthology resource based on 5090 organisms and 2502 viruses. Nucleic Acids Res. 2019;47(D1):D309–14.
45. Buchfink B, Reuter K, Drost H-G. Sensitive protein alignments at tree-of-life scale using DIAMOND. Nat Methods. 2021;18(4):366–8.
46. Deng Y, Jiang Y-H, Yang Y, He Z, Luo F, Zhou J. Molecular ecological network analyses. BMC Bioinf. 2012;13:1–20.
47. Deng Y, Jiang Y-H, Yang Y, He Z, Luo F, Zhou J. Molecular ecological network analyses. BMC Bioinform. 2012;13:1–20.
48. Bastian MHS, Jacomy M. Gephi: an open source software for exploring and manipulating networks. In: Third international AAAI conference on weblogs and social media. 2009.
49. Zhang J, Liu Y-X, Guo X, Qin Y, Garrido-Oter R, Schulze-Lefert P, Bai Y. High-throughput cultivation and identification of bacteria from the plant root microbiota. Nat Protoc. 2021;16(2):988–1012.
50. Kumar SSG, Li M, Knyaz C, Tamura K. MEGA X: molecular evolutionary genetics analysis across computing platforms. Mol Biol Evol. 2018;35(6):1547–9.
51. Bankevich A, Nurk S, Antipov D, Gurevich AA, Dvorkin M, Kulikov AS, Lesin VM, Nikolenko SI, Pham S, Prjibelski AD. SPAdes: a new genome assembly algorithm and its applications to single-cell sequencing. J Comput Biol. 2012;19(5):455–77.
52. Love MIHW, Anders S. Moderated estimation of fold change and dispersion for RNA-seq data with DESeq2. Genome Biol. 2014;15(12):550.
53. Zhao Z, Dai H, Wang G, Peng Y, Liao F, Wu J, Liang T. Carbon nanoparticles promoted the absorption of potassium ions by tobacco roots via regulation of K+ flux and ion channel gene expression. Curr Nanosci. 2024;20(3):390–8.
54. Lijuan C, Huibo H, Zuguo S, Jianli Y, Chang G, Lu D, Dongfei L. Effects of foliar application of carbon nanosol on growth of potted tobacco seedlings. J Henan Agric Sci. 2024;53(8):44.
55. Verma SK, Das AK, Patel MK, Shah A, Kumar V, Gantait S. Engineered nanomaterials for plant growth and development: a perspective analysis. Sci Total Environ. 2018;630:1413–35.
56. Zuverza-Mena N, Martínez-Fernández D, Du W, Hernandez-Viezcas JA, Bonilla-Bird N, López-Moreno ML, Komárek M, Peralta-Videa JR, Gardea-Torresdey JL. Exposure of engineered nanomaterials to plants: Insights into the physiological and biochemical responses-a review. Plant Physiol Biochem. 2017;110:236–64.
57. Feng Y, Wang C, Chen F, Cao X, Wang J, Yue L, Wang Z. Cerium oxide nanomaterials improved cucumber flowering, fruit yield and quality: the rhizosphere effect. Environ Sci Nano. 2023. https://doi.org/10.1039/D3EN00213F.
58. Jordan JT, Oates R, Subbiah S, Payton PR, Singh KP, Shah SA, Green MJ, Klein DM, Cañas-Carrell JE. Carbon nanotubes affect early growth, flowering time and phytohormones in tomato. Chemosphere. 2020;256: 127042.
59. Juárez-Maldonado AGT, Rubilar O, Fincheira P, Benavides-Mendoza A. Biostimulation and toxicity: the magnitude of the impact of nanomaterials in microorganisms and plants. J Adv Res. 2021;31:113–26.
60. Von Moos N, Slaveykova VI. Oxidative stress induced by inorganic nanoparticles in bacteria and aquatic microalgae–state of the art and knowledge gaps. Nanotoxicology. 2014;8(6):605–30.
61. Giorgetti L, Spanò C, Muccifora S, Bottega S, Barbieri F, Bellani L, Castiglione MR. Exploring the interaction between polystyrene nanoplastics and Allium cepa during germination: Internalization in root cells, induction of toxicity and oxidative stress. Plant Physiol Biochem. 2020;149:170–7.
62. Rajput VD, Minkina T, Sushkova S, Tsitsuashvili V, Mandzhieva S, Gorovtsov A, Nevidomskyaya D, Gromakova N. Effect of nanoparticles on crops and soil microbial communities. J Soils Sediments. 2018;18:2179–87.
63. Jangid K, Williams MA, Franzluebbers AJ, Schmidt TM, Coleman DC, Whitman WB. Land-use history has a stronger impact on soil microbial community composition than aboveground vegetation and soil properties. Soil Biol Biochem. 2011;43(10):2184–93.
64. Wang Z, Yue L, Dhankher OP, Xing B. Nano-enabled improvements of growth and nutritional quality in food plants driven by rhizosphere processes. Environ Int. 2020;142: 105831.
65. Mendes LW, Kuramae EE, Navarrete AA, Van Veen JA, Tsai SM. Taxonomical and functional microbial community selection in soybean rhizosphere. ISME J. 2014;8(8):1577–87.
66. Panke-Buisse K, Poole AC, Goodrich JK, Ley RE, Kao-Kniffin J. Selection on soil microbiomes reveals reproducible impacts on plant function. ISME J. 2015;9(4):980–9.
67. Richardson AE, Barea J-M, McNeill AM, Prigent-Combaret C. Acquisition of phosphorus and nitrogen in the rhizosphere and plant growth promotion by microorganisms. In.: Springer; 2009.
68. Taghavi S, Garafola C, Monchy S, Newman L, Hoffman A, Weyens N, Barac T, Vangronsveld J, van der Lelie D. Genome survey and characterization of endophytic bacteria exhibiting a beneficial effect on growth and development of poplar trees. Appl Environ Microbiol. 2009;75(3):748–57.
69. De Roy K, Marzorati M, Van den Abbeele P, Van de Wiele T, Boon N. Synthetic microbial ecosystems: an exciting tool to understand and apply microbial communities. Environ Microbiol. 2014;16(6):1472–81.
70. Ahmed T, Noman M, Gardea-Torresdey JL, White JC, Li B. Dynamic interplay between nano-enabled agrochemicals and the plant-associated microbiome. Trends Plant Sci. 2023. https://doi.org/10.1016/j.tplants.2023.06.001.
71. Finkel OM, Salas-González I, Castrillo G, Conway JM, Law TF, Teixeira PJPL, Wilson ED, Fitzpatrick CR, Jones CD, Dangl JL. A single bacterial genus maintains root growth in a complex microbiome. Nature. 2020;587(7832):103–8.
72. Moisan K, Cordovez V, van de Zande EM, Raaijmakers JM, Dicke M, Lucas-Barbosa D. Volatiles of pathogenic and non-pathogenic soil-borne fungi affect plant development and resistance to insects. Oecologia. 2019;190(3):589–604.
73. Lee S, Behringer G, Hung R, Bennett J. Effects of fungal volatile organic compounds on Arabidopsis thaliana growth and gene expression. Fungal Ecol. 2019;37:1–9.

74. Jain S, Varma A, Tuteja N, Choudhary DK. Bacterial volatiles in promotion of plant under biotic stress. Volatiles Food Sec. 2017;2017:299–311.
75. Lee S, Yap M, Behringer G, Hung R, Bennett JW. Volatile organic compounds emitted by Trichoderma species mediate plant growth. Fungal Biol Biotechnol. 2016;3(1):1–14.

Publisher's Note